

DECOLORIZATION OF METHYLENE BLUE AND METHYL ORANGE WITH Ag DOPED TiO₂ UNDER UV-A AND UV-VISIBLE CONDITIONS: PROCESS OPTIMIZATION BY RESPONSE SURFACE METHOD AND TOXICITY EVALUATION

ÇİFÇİ D.I.*

¹Department of Environmental Engineering
Çorlu Faculty of Engineering
Namik Kemal University, Çorlu 59860- Tekirdağ, TURKEY

Received: 17/01/2016

Accepted: 13/04/2016

Available online: 13/05/2016

*to whom all correspondence should be addressed:

e-mail: dicifci@nku.edu.tr

ABSTRACT

MB decolorization with pure TiO₂ and Ag doped TiO₂ based photocatalytic system were investigated under UV-A and UV-Visible conditions. Different ratios of Ag were used as metal dopant. 1% Ag-TiO₂ increased the decolorization efficiencies of MB and MO dyes, also the k_{app} constant enhanced under UV-A and UV-Visible conditions. A central composite analysis showed the effect of initial dye concentration, pH, Ag-TiO₂ concentration and the reaction time of photocatalytic process under UV-A irradiation in both dyes. The photocatalytic degradation pathways of both dyes by Ag doped TiO₂ catalyst were obtained in this study. According to these results, the application of Ag-TiO₂ catalyst are proved to be more effective than pure TiO₂ catalyst for both MB and MO removal. The toxicity test of *Daphnia Magna* shows that non toxic wastewater discharge to the receiving environment could be possible with photocatalytic degradation by Ag-TiO₂ catalyst.

Keywords: dye, decolorization, doped TiO₂, optimization, photocatalytic, toxicity.

1. Introduction

Different dyes applied in many industries such as textile, paint, ink, plastics and cosmetics processing are mostly poorly biodegradable pollutants and cause serious environmental problem due to the toxicity and carcinogenicity (Mirkhani *et al.*, 2009; Çifçi *et al.*, 2015). Advanced Oxidation Processes are commonly used to remove of dyes and toxic chemicals (Zhang *et al.*, 2014; Pekakis *et al.*, 2006). In recent years, doping metals (e.g. Pd, Au and Ag) on the surface of TiO₂ is one of the common methods applied to increase the photocatalytic activity of TiO₂ under visible light and sunlights (Sun *et al.*, 2014). Among the metals, silver has attracted intense attention to increase photocatalytic activity and stability and can act as electron traps aiding electron-hole separation (Arabatzis *et al.*, 2003). Researches showed the improving in the efficiency of some dyes with Ag doped TiO₂ (Padikkaparambil *et al.*, 2012; Mirkhani *et al.*, 2009). However, there are a few reasearches about the examination of the effects of process parameters by statistical methods. Response surface methodology (RSM) is very useful, quick and cost-effective statistical method that are obtained optimization of different parameters and exhibits the interaction of these parameters (Khataee *et al.*, 2010; Kasiri *et al.*, 2011; Barka *et al.*, 2014).

The aim of this study is to evaluate MB and MO decolorization by pure TiO₂ and Ag doped TiO₂/UV process and also examining the effects of initial dye concentration, pH, catalyst concentration and time on photocatalytic degradation by using response surface methodology. Also, toxicity is evaluated at optimum

conditions by *Daphnia Magna* and identified the intermediate products and degradation pathways of both dyes.

2. Materials and methods

2.1. Chemicals and analytical methods

Methylene blue (MB, Cat No: 1.05045), methyl orange (MO, Cat No: 1.01322), silver nitrate (AgNO_3 , Cat No: 1.01510), glacial acetic acid (Cat No: 1.00056), Ethanol (Cat No: 1.00986) hydrochloric acid (Cat No: 1.00314), and sodium hydroxide (Cat No: 1.06462) were purchased from Merck. Titanium (IV) butoxide (Cat No: 86910, purum $\geq 97.0\%$) was obtained from Fluka. All aqueous solutions were prepared by using deionized water. The determination of Methylene Blue (MB, $\lambda = 664 \text{ nm}$) and Methyl Orange (MO, $\lambda = 464 \text{ nm}$) at different irradiation times were analyzed by UV-vis spectroscopy in a Shimadzu UV-2401 PC instrument in standard quartz cells.

Residues and intermediates of MB and MO were determined by ESI-MS using an AB Sciex (Models 3200 QTRAP) and MS was operated in positive and negative ionization mode with electrospray source ionization (ESI). The positive ionization mode was operated under the following conditions: curtain gas (CUR): 20, ion spray voltage (IS): 5500, DP: 90 and EP: 10. The negative ionization mode was operated under the following conditions: curtain gas (CUR): 20, ion spray voltage (IS): -450, DP: -70 and EP: -12.

Pure and Ag doped TiO_2 catalysts were characterized by scanning electron microscope (SEM)-energy dispersive X-ray analyzer (EDX) and Fourier Transform Infrared Spectroscopy (FTIR). The particle morphology was observed by a scanning electron microscope (FEI-QUANTA FEG 250) with secondary electron detector (Everhardt Thornley ETD detector) operated at 5 kV, 2.5 spot and 60000x mag and equipped with an attachment for the Energy dispersive X-ray spectroscopy (EDX) was used for analysis of elemental compositions of the photocatalysts. FT-IR was performed at room temperature on a Bruker VERTEX 70 ATR and it was used to evaluate and identify the formation of functional groups formed during synthesis of the photocatalyst in the range of 400 to 4000 cm^{-1} . The pH_{pzc} of the samples was determined according to the literature (Asgari *et al.*, 2013).

2.2. Preparation of pure and doped TiO_2

Pure TiO_2 and Ag doped TiO_2 catalysts were prepared by sol-gel technique at room temperature. Ethanol was slowly added to titanium (IV) butoxide and was stirred for 60 min (Ethanol: Titanium Butoxide: 10:1 v/v). A second solution was prepared mixing glacial acetic acid with deionized water (Glacial acetic acid: Distilled water: 1:3 v/v) and this solution was gradually added to titanium (IV) butoxide and ethanol solution and stirring continued for one hour. Ag- TiO_2 ratios (weight%) were selected as 0.5, 1.0, 1.5 and 2.0% Ag (weight%) was added glacial acetic acid and deionized water solutions for Ag doped TiO_2 . After that sol was dried at 105 °C for 12 hours and calcinated in muffle furnace at 450 °C for 2 hours. Pure TiO_2 was prepared by the same methods of metal doped TiO_2 without any metal additions.

2.3. Photocatalytic experiments

The photocatalytic experiments performed with 150 mL quartz beaker and carried out at Luzchem UV Photoreactor equipped with fifteen UV-A (Hitachi, 8W) or UV-Vis light lamps (Sylvania, 8W) at 30°C. Samples for analysis were collected at 3 ml and through 0.45 μm cellulose acetate membranes. NaOH and HCl solutions were used for pH adjustments in this study.

2.4. Central composite design (CCD)

CCD were used to evaluate the influence of operating parameters and to determine the optimum Ag/ TiO_2 ratios for photodegradation of MB and MO. The CCD matrix was used in the experiments and designed by using the Design Expert. Four factors were investigated as initial MB or MO concentration (mg l^{-1}), pH, catalyst concentration (g l^{-1}) and reaction time (min.). Total number of experiments was 30 and the experimental design points consists of 2^n factorial points ($2^4 = 16$), $2n$ axial points ($2 \times 4 = 8$) and 6 replications

of central points (Table 1). The second-order polynomial equation was used in this study according to previous research (Zuorro *et al.*, 2013).

Table 1. Experimental factors and levels in the central composite design.

Factors	Levels				
	-2	-1	0	+1	+2
MB or MO Concentration (mg l ⁻¹) (X ₁)	5	10	15	20	25
pH (X ₂)	3	5	7	9	11
Ag-TiO ₂ Concentration (mg l ⁻¹) (X ₃)	0.125	0.25	0.375	0.50	0.625
Reaction time (min ⁻¹) (X ₄)	30	60	90	120	150

2.4. Toxicity by *Daphia Magna*

Acute toxicity of initial and photocatalytic treated samples of different times were done by *Daphnia magna* (new born daphnids <24 h) according to ISO 6341 Method (1996). Toxicity tests details were given at Cifci *et al.*, 2015. All samples were diluted by 50% and set at pH 8, also 20 ml effective volume was used in the test beaker.

3. Results and discussion

3.1. Characterization of pure TiO₂ and doped TiO₂ catalyst

Figure 1 shows the SEM images of pure TiO₂ and 0.5, 1.0 and 2.0% Ag doped TiO₂ particles. All the morphologies of particles have different shapes of grains with irregular boundaries and exhibit aggregated particles with many smaller crystals. It can be seen that in 2.0% Ag-TiO₂ nanoparticles have increased the particle size of TiO₂ nanoparticles. The results of EDX analysis for elemental composition of pure TiO₂ and 0.5, 1.0 and 2.0% Ag-TiO₂ showed that the weight of Ti (titanium) and O (oxygen) were the main components of the nanoparticles. The atomic ratio of Ti and O in the nanoparticles were within the range of 8.7-10.5% and 90.1-91.3%, respectively. The atomic ratio of Ag in the 0.5, 1.0 and 1.5% Ag-TiO₂ were obtained 0.11%, 0.20% and 0.44%, respectively.

According to the FT-IR spectra of nanoparticles, four significant peaks were shown at ca. 400-500, 600-800, 1600-1700 and 2300-2400 cm⁻¹. The peak around 400-500 cm⁻¹ assigned to the characteristic vibrations of Ti-O-Ti lattice and bending mode of vibrations and at ca. 700 and 800 cm⁻¹ were attributed to the stretching vibrations of Ti-O bonds in the TiO₂ lattice (Bezrodna *et al.*, 2004). Peak around 1600-1700 cm⁻¹ represented the bending vibrations of the O-H bending which adsorb hydroxyl ions on the surface of catalyst plays an important role in increasing photocatalytic activity. Comparing the FT-IR spectra of the pure and Ag doped TiO₂, significant changes were observed at peaks around 600-800, 1600-1700 and 2300-2400 cm⁻¹ when Ag doped the TiO₂ surface. The peaks increased with escalating Ag weight from 0.5% to 1.0%; however in 2.0% Ag-TiO₂ nanoparticles peaks decreased according to 1.0% Ag-TiO₂ nanoparticles. Furthermore, with doping Ag on to TiO₂ catalyst, there has become a new peak at around 1500-1600 cm⁻¹.

pH_{pzc} values of Ag-TiO₂ did not significantly change between 0-1% Ag-TiO₂ and they were 6.6, 6.33 and 6.25 in TiO₂, 0.5% Ag-TiO₂ and 1.0% Ag-TiO₂. However, at 2.0% Ag-TiO₂ pH_{pzc} values increased to 7.05. pH_{pzc} value is important due to positively surface charged (pH < pH_{pzc}) and negatively surface charged (pH > pH_{pzc}) of the particles (Khanna and Shetty, 2013).

3.2. Photocatalytic activity of MB and MO

In the study, photolysis can be ignored due to very low degradation of MB and MO in the absence of catalysts under UV-A conditions. MB removal efficiencies were not significantly changed by 0.5% Ag-TiO₂ while it was increased from %83 to %99 with %1 Ag doped the TiO₂ catalyst. A similar result was also observed on MO removal. However, the MB or MO decolorization efficiencies decreased both UV-A and UV-Visible conditions when Ag amount increase than 1.0%. The high amount of Ag particles on the TiO₂ surface decrease the intensity of light through photocatalytic degradation. As a consequence, maximum

MB and MO decolorization were achieved at 1.0% Ag-TiO₂. Moreover, the irradiation time decreased from 120 min. to 90 min with 1.0% Ag/TiO₂ catalyst under UV-A conditions.

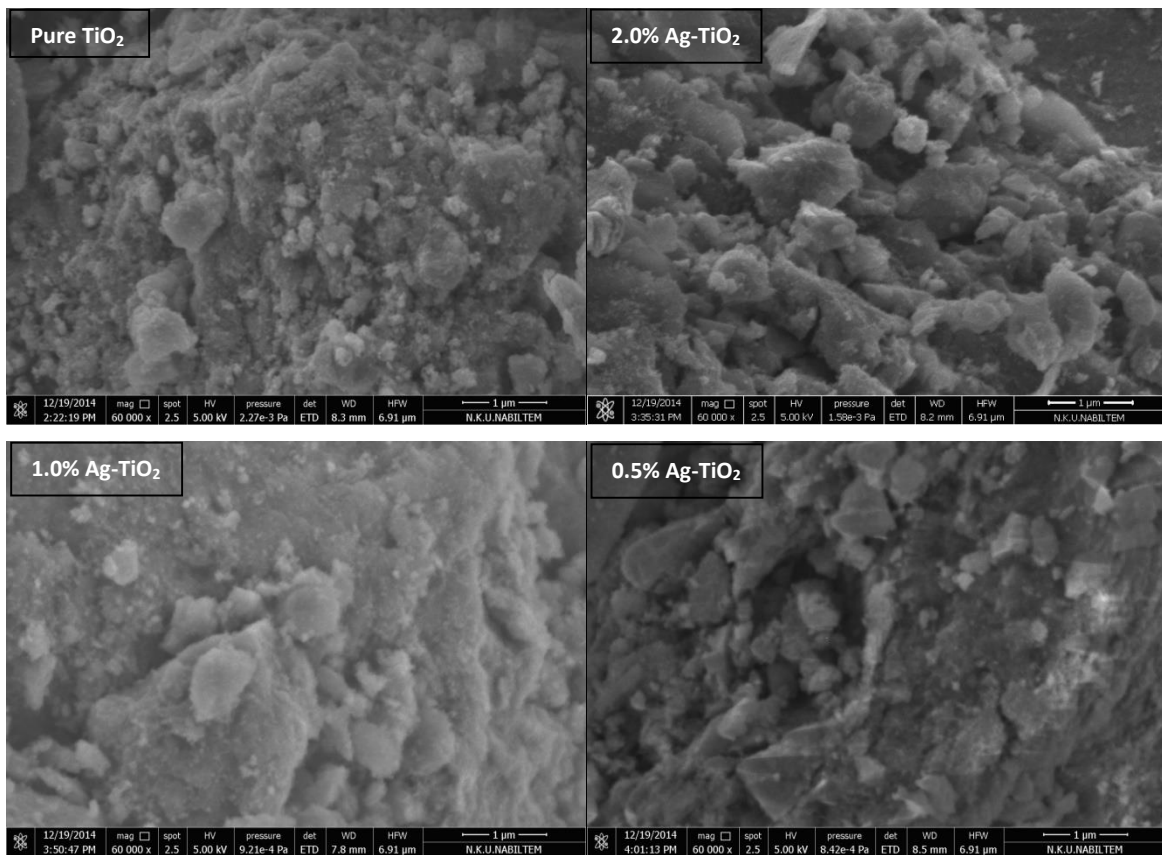


Figure 1. SEM images of pure TiO₂ and 2.0, 1.0 and 0.5% Ag-TiO₂ nanoparticles

In UV-Visible conditions, MB decolorization increased from 18% to 44% after 7 h. irradiation with 1% Ag-TiO₂ nanoparticles while MO decolorization increased from 27% to 36%. Photocatalytic degradation of MB and MO were fitted to pseudo first order reaction kinetics for TiO₂/UV process. Pseudo first order kinetics were calculated according to Zaharieva *et al.*, 2015 and pseudo first order kinetic constants are given as k_{app} . According to results, k_{app} was obtained approximately 2 fold higher with 1.0% Ag-TiO₂ than pure TiO₂ catalyst in MB decolorization while its 3.5 fold higher in MO decolorization.

Table 2. MO and MB kinetics of Ag-TiO₂ catalyts under UV-A and UV-Vis conditions (MB or MO: 20 mg l⁻¹, pH 7.0, catalyst: 0.5 g l⁻¹)

Catalyst	UV-A for MB		UV-Visible for MB		UV-A for MO		UV-Visible for MO	
	k_{app} *	Removal	k_{app}	Removal	k_{app} *	Removal	k_{app}	Removal
TiO ₂	15.0	83.1	0.54	18.3	9.3	80.4	0.70	26.8
0.5% Ag-TiO ₂	14.4	81.5	0.70	24.3	11.9	82.6	0.54	25.4
1.0 % Ag-TiO ₂	34.1	99.2	1.41	44.5	33.2	99.6	1.02	36.5
1.5% Ag-TiO ₂	25.7	96.8	0.84	30.6	17.0	95.4	0.85	34.8
2.0% Ag-TiO ₂	22.7	95.1	0.73	25.9	14.8	92.8	0.63	29.5

* k_{app} values are min⁻¹ *10⁻³ and Removal is %

3.3. Analysis of central composite design

Maximum photodegradation of MB and MO were found at the 1.0% weight ratio of Ag-TiO₂ catalyst and CCD experiment were done in photocatalytic degradation of MB and MO with UV-A conditions. The experimental and predicted results of MB and MO removal with variable matrix were shown in Table 3.

In the CCD experimental and predicted datas of Ag-TiO₂/UV-A process, the results of the quadratic regression model are fitted analysis of variance (ANOVA) at 95% confidence level ($p < 0.05$). The Model F-value (15-18) and P value Prob > F (< 0.0001) imply that the model is significant. The larger the magnitude of the t-value and smaller the P-value, the more significant is the corresponding coefficient (Liu and Chiou, 2005). Moreover, the value of the determination coefficient (R^2) and the adjusted determination coefficient (adjusted R^2) are obtained 0.9519 and 0.9070 in MB decolorization and 0.9599 and 0.9225 in MO decolorization, respectively and it is recommended that R^2 should be more than 0.80 to fit the regression model (Daghrir *et al.*, 2013). The closing experimentals and predicted values are means that the model is a good fit in these experiments. MB and MO decolorization equations are given in Eq. 1 and Eq. 2, respectively.

Table 3. Experimental design matrix and response based on experimental and predicted value on MB and MO removal efficiency

Standard Order	X ₁	X ₂	X ₃	X ₄	MB Removal (%)		MO Removal (%)	
					Experimental	Predicted	Experimental	Predicted
1	-1	-1	-1	-1	53.6	57.8	78.5	81.0
2	1	-1	-1	-1	74.7	68.4	50.6	49.1
3	-1	1	-1	-1	96.3	96.7	71.0	69.0
4	1	1	-1	-1	74.0	77.1	33.8	37.6
5	-1	-1	1	-1	42.9	47.6	90.8	90.1
6	1	-1	1	-1	60.7	59.8	79.9	84.1
7	-1	1	1	-1	99.6	99.9	75.7	78.6
8	1	1	1	-1	79.2	82.0	78.6	73.2
9	-1	-1	-1	1	75.8	75.7	99.2	99.6
10	1	-1	-1	1	88.9	86.8	72.6	69.9
11	-1	1	-1	1	100.0	99.0	96.8	92.8
12	1	1	-1	1	82.0	80.1	67.9	63.6
13	-1	-1	1	1	77.2	72.3	98.1	94.6
14	1	-1	1	1	82.7	85.1	93.9	90.8
15	-1	1	1	1	100.0	109.0	91.9	88.4
16	1	1	1	1	97.7	91.8	87.5	85.2
17	-2	0	0	0	100.0	94.2	93.5	95.1
18	2	0	0	0	82.6	87.5	56.8	60.0
19	0	-2	0	0	45.6	47.6	84.2	84.0
20	0	2	0	0	96.0	93.1	61.4	66.4
21	0	0	-2	0	69.5	71.8	53.2	54.8
22	0	0	2	0	76.5	73.3	82.1	85.4
23	0	0	0	-2	78.5	74.8	78.0	73.8
24	0	0	0	2	99.6	102.4	95.3	100.3
25	0	0	0	0	94.1	93.5	93.1	93.3
26	0	0	0	0	93.1	93.5	93.4	93.3
27	0	0	0	0	94.1	93.5	93.7	93.3
28	0	0	0	0	92.9	93.5	93.5	93.3
29	0	0	0	0	93.1	93.5	93.4	93.3
30	0	0	0	0	93.6	93.5	92.6	93.3

X₁ MB or MO Concentration (mg l⁻¹), X₂ pH, X₃ Ag-TiO₂ Concentration (g l⁻¹), X₄ Reaction time (min)

The expression of MB decolorization percentage by following equation:

$$Y=93.46-1.68*X_1+11.38*X_2+0.37*X_3+6.90*X_4-7.52*X_1X_2+0.42*X_1X_3+0.14*X_1X_4+3.36*X_2X_3-3.88*X_2X_4+1.70*X_3X_4-0.66*X_1^2-5.78*X_2^2-5.23*X_3^2-1.22*X_4^2$$

(1)

According to Equation 1, pH value of solution affects the MB removal efficiency more than the other parameters and pH (X_2) and time (X_4) are important factors on MB decolorization. pH (X_2), Ag-TiO₂ concentration (X_3) and time (X_4) have positive effect on the photocatalytic degradation of MB. It means that the photocatalytic degradation is the most suitable at high pH, high Ag-TiO₂ concentration and high reaction time (Fig. 2). Besides, MB removal decreased while the initial MB concentration (X_1) increased. Also, quadratic effect is observed in pH and Ag-TiO₂ concentration and synergy effect is observed between initial MB concentration and pH; pH and Ag-TiO₂ concentration; pH and time. MB removal efficiency is decreasing from 100% to 60% at low Ag-TiO₂ concentration and acidic conditions. MB removal obtained about 70% even increasing Ag-TiO₂ concentration from 0.125 to 0.625 g l⁻¹ at pH 3. However, it could be increased to 90% with increasing pH to 9 at low Ag-TiO₂ concentration (0.25 g l⁻¹).

The expression of MO decolorization percentage by following equation:

$$Y=93.27-8.79*X_1-4.42*X_2+7.65*X_3+7.64*X_4+0.13*X_1X_2+6.49*X_1X_3+0.56*X_1X_4+0.16*X_2X_3+1.32*X_2X_4-3.51*X_3X_4-3.93*X_1^2-4.52*X_2^2-5.80*X_3^2-1.06*X_4^2$$

(2)

According to Equation 2, all factors have most effect on the response factors of MO decolorization and the effect of the independent parameters is counted as: initial MO concentration > Ag-TiO₂ concentration > oxidation time > pH. A similar result was obtained at other research and it is explained that high dye concentration caused the reduction of penetration (Sahoo and Gupta, 2012). Ag-TiO₂ concentration (X_3) and time (X_4) have positive effects on the photocatalytic degradation of MO, while the initial MB concentration (X_1) and pH (X_2) have negative. It means that the photocatalytic degradation is the most suitable at low initial MO concentration, low pH, high Ag-TiO₂ concentration and high reaction time (Fig. 3). The most important parameter to enhance the MO removal efficiency is initial MO concentration and the effects of Ag/TiO₂ and oxidation time are very close to the effects initial MO concentration. Besides, quadratic effect is observed in the initial MO concentration, pH and Ag-TiO₂ concentration and synergy effect is observed between initial MO concentration and Ag-TiO₂ concentration; Ag-TiO₂ concentration and reaction time. MO removal efficiency is decreased to 60% when pH 9 and Ag-TiO₂ concentration 0.25 g l⁻¹ or pH 9 and 60 min oxidation time.

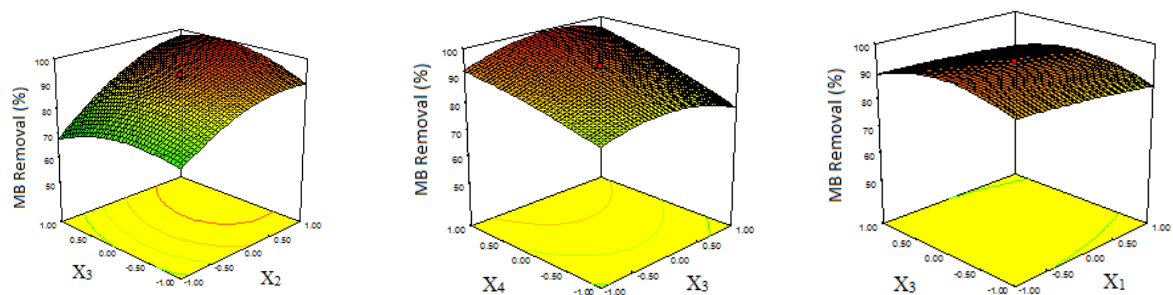


Figure 2. Response surface and contour plots of MB decolorization (%) between independent variables

MB and MO removal efficiencies decrease by increasing the initial MB and MO concentration. High MB decolorization was observed at 5, 10 and 15 mg l⁻¹ MB concentration than 20 and 25 mg l⁻¹ MB concentration. Xiao *et al.* (2008) observed similar trends and MB degradation was decreased at 20 and 50 mg l⁻¹ than 5 and 10 mg l⁻¹ MB concentration. High MB concentrations cause the reduction of light penetration into solution and inhibit photogenerated holes or absorb UV photons by the pollutants instead of TiO₂ photocatalyst (Xiao *et al.*, 2008; Dagherir *et al.*, 2013). Besides, according to MB removal, MO removal efficiency is affected more than the increase of MO concentration. MO removal efficiency was decreased to 56.8% at 25 mg l⁻¹ MO concentration while MB removal efficiency is 79.5% at 25 mg l⁻¹ MB concentration.

Photocatalytic decolorization efficiency of MB increased with increasing the pH value and similar trends were observed in the literature (Xiao *et al.*, 2008; Lin *et al.*, 2006). Besides, the adsorption of MB increased with increasing pH (Lachheb *et al.*, 2002). In this study, maximum MB decolorization was observed at pH 9. On the other hand, maximum MO decolorization was observed in acidic condition at pH 5.

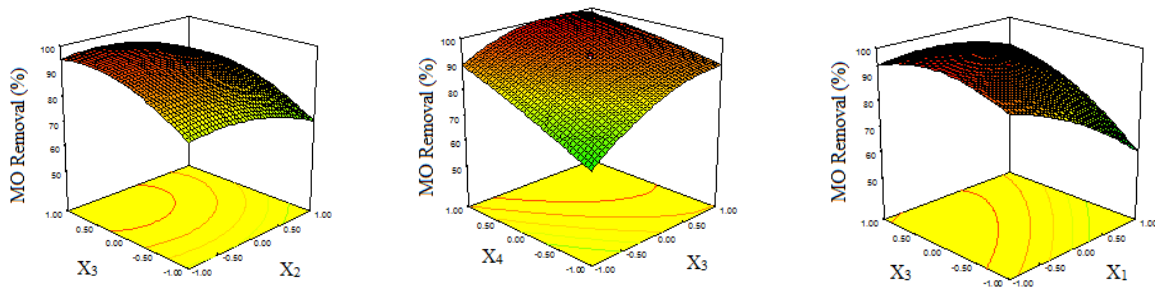


Figure 3. Response surface and contour plots of MO decolorization (%) between four independent variables at central level

The influence of Ag/TiO₂ concentration, within the range of 0.125–0.625 g l⁻¹ is evaluated and the MB removal rate increased with the increasing Ag-TiO₂ concentration until 0.500 g l⁻¹. After 120 min irradiation, 71.9% MB decolorization efficiency was observed at 0.125 g l⁻¹ Ag-TiO₂ concentration and it increased to 99.6% MB removal at 0.375 g l⁻¹ Ag-TiO₂ concentration while it is slightly decreased to 93.4% MB removal at 0.625 g l⁻¹ Ag-TiO₂ concentration. When the initial MB or MO concentrations increase, the reaction time increases in parallel due to the reducing the photogeneration of holes or OH radicals on the surface of catalyst.

3.4. Toxicity Evaluation at optimum conditions

Photocatalytic oxidation process must be evaluated by toxicity due to the understanding full of minerilization or the toxicity of intermediate by-products (Saien and Khezrianjoo, 2008). Toxicity assays by *Daphnia Magna* is benefical method for evaluation of toxicity in textile wastewater or dyes (Meriç *et al.*, 2005a; 2005b). Optimum conditions of MB and MO were selected to evaluate of toxicity by photocatalytic process. Toxicity of *Daphnia Magna* decreased with degrading the dye molecules in time and there was no observed toxicity after 60 min oxidation time while approximately 98-99% MB or MO removal and %38-40 TOC removal observed after 60 min photocatalytic oxidation. However, TOC removal was increased with oxidation time increased from 60 to 120 min and TOC removal was obtained as 83.3% for MO, while it is observed that 45.8% of TOC removal for MB after 120 min photocatalytic oxidation time (Fig. 4).

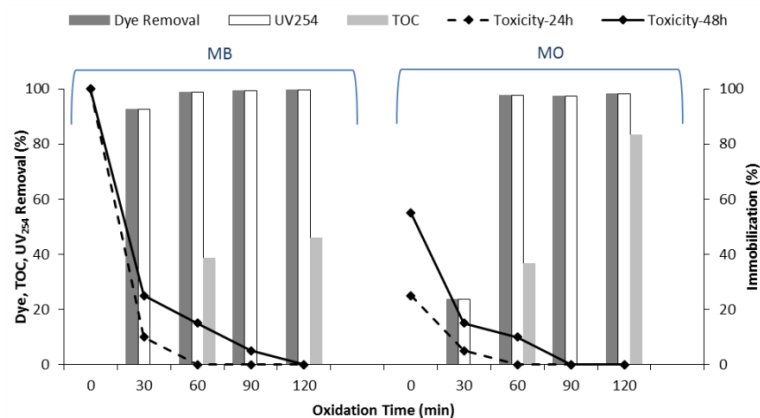


Figure 4. Decolorization and toxicity evaluation of optimum condition of MB (MB: 20 mg l⁻¹, pH: 9 and Ag-TiO₂: 0.375 g l⁻¹) and MO (MO: 20 mg l⁻¹, pH: 5 and Ag-TiO₂: 0.625 g l⁻¹)

Decreasing *Daphnia Magna* immobilization with increasing oxidation time in both MB and MO dyes indicate that breaking of the long chain molecules of dyes and occurred nontoxic by-products (Meriç *et al.*, 2005b). Besides, more than 95% UV₂₅₄ removal showed the high dearomatization in both systems (Çifçi *et al.*, 2015).

3.3. Paracetamol Residues in treated samples by Ag doped TiO₂ catalysts

ESI-MS analysis was used to determine the aromatic by-products of MB and MO photo-oxidation and both of MB and MO degradation pathways are given in Figure 5 a-b. The MS analysis gives six significant m/z values which are 114.1, 101.7, 140.1, 123.9, 288.1 and 107.9 m/z in MB degradation while it is four significant m/z values which are 101.9, 240.7, 114.1 and 140.1 m/z in MO degradation.

MB was degraded to single ring structure products and three main single ring structure by-products were observed in the sample which were at 124 m/z (aminoquinone), 108 m/z (benzoquinone) and 140 m/z (Phenylsulfinate ion). Phenylsulfinate ion at 140 m/z was also observed photocatalytic degradation of methylene blue on nanocrystalline TiO₂ (Gnaser *et al.*, 2005).

MO was separated into two forms due to the hydroxyl radical attack the benzene containing SO₃ group and phenylsulfinate ion at 140 m/z was observed in the treated samples like MB treated samples. On the other hand, product at 241 m/z could be MO molecules (absence of SO₃) which was given in literature (Baiocchi *et al.*, 2002). Aromatic structure of intermediates generate demethylation reactions by hydroxyl radicals and the molecule at 212 m/z (both methyl groups absence) was observed as by oxidation products (Mascolo *et al.*, 2007; Baiocchi *et al.*, 2002). After the separation of methyl groups, the OH radicals attack has become to take place on the –N=N– double bond and the aromatic rings of products were degrading to single ring structures such as at 124 m/z (aminoquinone) and 108 m/z (benzoquinone).

114.1 and 101.7 m/z values were observed in both of the dyes which indicated that intermediates were degrading to smaller molecules such as carboxylic acids group. At the end of the degradation of dyes, these carboxylic acids converted to inorganic ions such as carbon dioxide, nitrate, sulfate, water and chlorine (Huang *et al.*, 2010; Ghauch *et al.*, 2012).

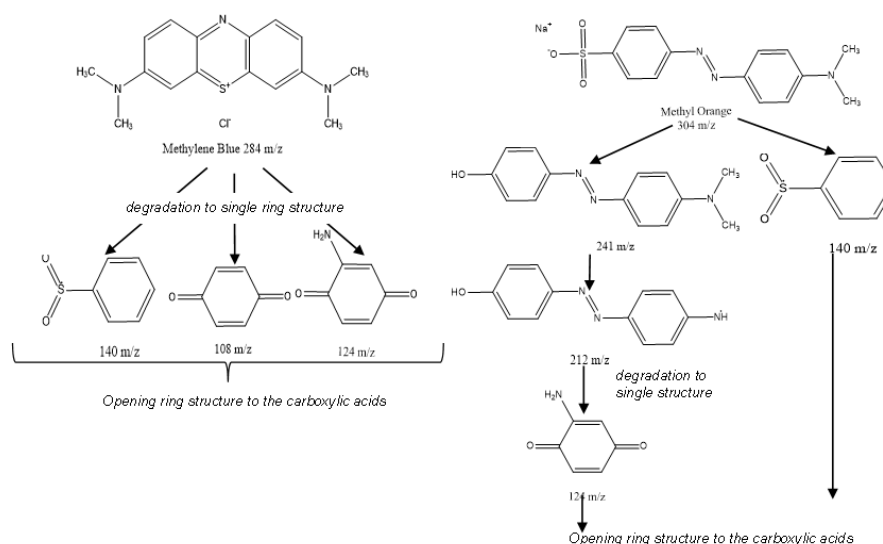


Figure 5. Possible degradation pathway of dyes by Ag doped TiO₂ MB (MB: 20 mg l⁻¹, pH: 9 and Ag-TiO₂: 0.375 g l⁻¹, oxidation time: 120 min) and MO (MO: 20 mg l⁻¹, pH: 5 and Ag-TiO₂: 0.625 g l⁻¹, oxidation time: 120 min)

4. Conclusion

In this study, photocatalytic degradation of methylene blue and methyl orange by using pure TiO₂ and Ag-TiO₂ were evaluated. Maximum MB decolorization was observed 1% Ag-TiO₂/UV-A process and it was

found that 1% (weight) Ag doped TiO₂ increased both the MB and MO removal efficiency from about 80% to 99% at 0.5 g l⁻¹ catalyst concentration after 2 hour photocatalytic degradation. Furthermore, MB and MO photodegradation reaction kinetic constant increased approximately 2 and 3.5 fold higher by doping 1% Ag on the surface of TiO₂ at TiO₂/UV process, respectively. The toxicity of Daphnia Magna was not observed in both dyes by Ag-TiO₂ catalyst after 2 h photocatalytic oxidation times and this means that both of the dyes can be degraded to non toxic degradation products. Also, it was examined that the effects of the initial MB concentration, pH, Ag-TiO₂ concentration and reaction time on MB decolorization in Ag-TiO₂/UV-A process. In MB decolorization, pH was the most important parameter for the photodegradation while initial MO concentration was the most effect the photocatalytic process in MO decolorization. The Response Surface Methodology approach was a useful method for estimation of the influence process operating conditions on MB and MO photodegradation. Metal doped TiO₂ could be enhanced the photocatalytic degradation of dyes and the residues products were the non toxic in aquatic environment.

Funding

This study was financed by Namik Kemal University Scientific Research Projects with project number NKUBAP.00.17.AR.14.01.

References

- Arabatzis I.M., Stergiopoulos T., Bernard M.C., Labou D., Neophytides S.G. and Falaras P. (2003), Silver-modified titanium dioxide thin films for efficient photodegradation of methyl orange, *Applied Catalysis B: Environmental*, **42**, 187-201.
- Asgari G., Mohammadi A.S., Mortazavi S.B. and Ramavandi B. (2013), Investigation on the pyrolysis of cow bone as a catalyst for ozone aqueous decomposition: Kinetic approach, *Journal of Analytical and Applied Pyrolysis*, **99**, 149-154.
- Barka N., Abdennouri M., Boussaoud A., Galadi A., Baâlala M., Bensitel M., Sahibed-Dine A., Nohair K. and Sadiq M. (2014), Full factorial experimental design applied to oxalic acid photocatalytic degradation in TiO₂ aqueous suspension, *Arabian Journal of Chemistry*, **7**(5), 752-757.
- Baiocchi C., Brussino M.C., Pramauro E., Prevot A.B., Palmisano L. and Marci G. (2002), Characterization of methyl orange and its photocatalytic degradation products by HPLC/UV-VIS diode array and atmospheric pressure ionization quadrupole ion trap mass spectrometry, *International Journal of Mass Spectrometry*, **214**, 247-256.
- Bezrodna T., Puchkovska G., Shymanovska V., Baran J. and Ratajczak H. (2004), IR-analysis of H-bonded H₂O on the pure TiO₂ surface, *Journal of Molecular Structure*, **700**, 175-181
- Çifçi D.I. and Meriç S. (2015), Optimization of Suspended photocatalytic treatment of two biologically treated textile effluents using TiO₂ and ZnO catalysts, *Global NEST Journal*, **17**(4), 653-663.
- Daghrir R., Drogui P., Dimboukou-Mpira A. and El Khakani M.A. (2013), Photoelectrocatalytic degradation of carbamazepine using Ti/TiO₂ nanostructured electrodes deposited by means of a pulsed laser deposition process, *Chemosphere*, **93**, 2756-2766.
- Ghauch A., Tuqan A.M., Kibbi N. and Geryes S. (2012), Methylene blue discoloration by heated persulfate in aqueous solution, *Chemical Engineering Journal*, **213**, 259-271.
- Gnaser H., Savina M.R., Calaway W.F., Tripa C.E., Vervovkin I.V. and Pellin M.J. (2005), Photocatalytic degradation of methylene blue on nanocrystalline TiO₂: Surface mass spectrometry of reaction intermediates, *International Journal of Mass Spectrometry*, **245**, 61-67
- Huang F., Chen L., Wang H. and Yan Z. (2010), Analysis of the degradation mechanism of methylene blue by atmospheric pressure dielectric barrier discharge plasma, *Chemical Engineering Journal*, **162**, 250-256.
- ISO 6341 Method (1996) International Organization for Standardization, Water Quality: Determination of the Inhibition of the Mobility of Daphnia magna Straus (Cladocera, Crustacea) - Acute Toxicity Test. ISO 6341, International Organization of Standardization, Geneva, Switzerland.
- Kasiri M.B. and Khataee A.R. (2011), Photooxidative decolorization of two organic dyes with different chemical structures by UV/H₂O₂ process: Experimental design, *Desalination*, **270**, 151-159.

- Khanna A. and Shetty V.K. (2013), Solar photocatalysis for treatment of Acid Yellow-17 (AY-17) dye contaminated water using Ag@TiO₂ core-shell structured nanoparticles, *Environmental Science Pollution Research*, **20**, 5692-5707.
- Khataee A.R., Fathinia M., Aber S. and Zarei M. (2010), Optimization of photocatalytic treatment of dye solution on supported TiO₂ nanoparticles by central composite design: Intermediates identification, *Journal of Hazardous Materials*, **181**, 886-897.
- Lachheb H., Puzenat E., Houas A., Ksibi M., Elaloui E., Guillard C. and Herrmann J.-M. (2002), Photocatalytic degradation of various types of dyes (Alizarin S, Crocein Orange G, Methyl Red, Congo Red, Methylene Blue) in water by UV-irradiated titania, *Applied Catalysis B: Environmental*, **39**, 75-90.
- Lin X.P., Huang F.Q., Wang W.D. and Zhang K.L. (2006), A novel photocatalyst BiSbO₄ for degradation of methylene blue, *Applied Catalysis A: General*, **307**(2), 257-262.
- Liu H.L. and Chiou Y.R. (2005), Optimal decolorization efficiency of Reactive Red 239 by UV/TiO₂ photocatalytic process coupled with response surface methodology, *Chemical Engineering Journal*, **112**, 173-179
- Mascolo G., Comparelli R., Curri M.L., Lovecchio G., Lopez A. and Agostiano A. (2007), Photocatalytic degradation of methyl red by TiO₂: Comparison of the efficiency of immobilized nanoparticles versus conventional suspended catalyst, *Journal of Hazardous Materials*, **142**(1-2), 130-137.
- Meriç S., Selcuk H., Gallo M. and Belgiorno V. (2005a), Decolourisation and detoxifying of Remazol Red dye and its mixture using Fenton's reagent, *Desalination*, **173**, 239-248.
- Meriç S., Selcuk H. and Belgiorno V. (2005b), Acute toxicity removal in textile finishing wastewater by Fenton's oxidation, ozone and coagulation-flocculation process, *Water Research*, **39**(6), 1147-1153.
- Mirkhani V., Tangestaninejad S., Moghadam M., Habibi M.H. and Rostami-Vartooni A. (2009), Photocatalytic degradation of azo dyes catalyzed by Ag doped TiO₂ Photocatalyst, *Journal of Iranian Chemical Society*, **6**(3), 578-587
- Padikkaparambil S., Yaakob Z., Narayanan B.N., Ramakrishnan R. and Viswanathan S. (2012), Novel preparation method of nanosilver doped sol gel TiO₂ photocatalysts for dye pollutant degradation, *Journal of Sol-Gel Science Technology*, **63**, 108-115.
- Pekakis P.A., Xekoukoulotakis N.P. and Mantzavinos D. (2006), Treatment of textile dyehouse wastewater by TiO₂ photocatalysis, *Water Research*, **40**(6), 1276-1286.
- Sahoo C. and Gupta A.K. (2012), Optimization of photocatalytic degradation of methylene blue using silver ion doped titanium dioxide by combination of experimental design and response surface approach, *Journal of Hazardous Materials*, **215-216**, 302-310.
- Sun J., Liu N., Xiao Z., An Q. and Huang D. (2014), Gold-Titania/protonated zeolite nanocomposite photocatalysts for methyl orange degradation under ultraviolet and visible irradiation, *Materials Science in Semiconductor Processing*, **25**, 286-293.
- Saien J. and Khezrianjoo S. (2008), Degradation of the fungicide carbendazim in aqueous solutions with UV/TiO₂ process: Optimization, kinetics and toxicity studies, *Journal of Hazardous Materials*, **157**, 269-276
- Xiao Q., Zhang J., Xiao C., Si Z. and Tan X. (2008), Solar photocatalytic degradation of methylene blue in carbon-doped TiO₂ nanoparticles suspension, *Solar Energy*, **82**, 706-713.
- Zaharieva K., Rives V., Tsvetkov M., Cherkezova-Zheleva Z., Kunev B., Trujillano R., Mitov I. and Milanova M. (2015), Preparation, characterization and application of nanosized copper ferrite photocatalysts for dye degradation under UV irradiation, *Materials Chemistry and Physics*, **160**, 271-278.
- Zhang J., Zhang L., Zhou S., Chen H., Zhong H., Zhao Y. and Wang X. (2014), Magnetically separable attapulgite TiO₂Fe_xO_y composites with superior activity towards photodegradation of methyl orange under visible light radiation, *Journal of Industrial and Engineering Chemistry*, **20**(5), 3884-3889.
- Zuorro A., Fidaleo M. and Lavecchia R. (2013), Response surface methodology (RSM) analysis of photodegradation of sulfonated diazo dye Reactive Green 19 by UV/H₂O₂ process, *Journal of Environmental Management*, **127**, 28-35.